

Anomalous electronic Raman scattering in $\text{Na}_x\text{CoO}_2 \cdot y\text{H}_2\text{O}$

P. Lemmens^{1,2}, K.Y. Choi^{3,4}, V. Gnezdilov⁵, E.Ya.

Sherman⁶ D.P. Chen¹, C.T. Lin¹, F.C. Chou⁷, B. Keimer¹

¹ *Max Planck Inst. for Solid State Research, D-70569 Stuttgart, Germany*

² *Inst. for Physics of Condensed Matter,*

TU Braunschweig, D-38106 Braunschweig, Germany

³ *2. Physikalisches Inst., RWTH Aachen, D-52056 Aachen, Germany*

⁴ *Inst. for Materials Research, Tohoku University, Sendai 980-8577, Japan*

⁵ *B. I. Verkin Inst. for Low Temperature Physics, NASU, 61164 Kharkov, Ukraine*

⁶ *Dept. of Physics, Univ. of Toronto, Toronto ON, M5S 1A7, Canada*

⁷ *Center for Materials Science and Engineering,*

MIT, Cambridge, MA 02139, USA

(Dated: June 18, 2021)

Abstract

Raman scattering experiments on $\text{Na}_x\text{CoO}_2 \cdot y\text{H}_2\text{O}$ single crystals show a broad electronic continuum with a pronounced peak around 100 cm^{-1} and a cutoff at approximately 560 cm^{-1} over a wide range of doping levels. The electronic Raman spectra in superconducting and non-superconducting samples are similar at room temperature, but evolve in markedly different ways with decreasing temperature. For superconducting samples, the low-energy spectral weight is depleted upon cooling below $T^* \sim 150 \text{ K}$, indicating an opening of a pseudogap that is not present in non-superconducting materials. Weak additional phonon modes observed below T^* suggest that the pseudogap is associated with charge ordering.

PACS numbers: 72.80.Ga, 75.30.-m, 71.30.+h, 78.30.-j

The hydrated cobaltate $\text{Na}_x\text{CoO}_2 \cdot y\text{H}_2\text{O}$ has recently been in the focus of research on correlated electron systems, because it enables investigations of the relationship between superconductivity (SC)¹ and magnetic ordering on a triangular lattice^{2,3}. Electronic correlations can be tuned either by changing the Na content, leading to long-range antiferromagnetic order for $0.75 \leq x \leq 0.85$ ($T_N = 20$ K)^{4,5} and a metal-insulator transition at $x=1/2$ ^{6,7}, or by hydration leading to superconductivity^{1,8} in Na-poor samples with $x \sim 1/3$ and $y \sim 4/3$.

For Na-rich cobaltates, angle-resolved photoemission experiments^{9,10} show a large hole-like, hexagonal Fermi surface dominated by Co t_{2g} states of a_g symmetry^{11,12,13}. Several anomalies are observed in this doping range and for temperatures below approximately 150 K. Among them are a break in a weakly dispersing quasiparticle band at an energy of ~ 70 meV $\equiv 560$ cm⁻¹, which was attributed to a bosonic mode of electronic or lattice origin^{9,10}; a T-linear resistivity; a colossal thermopower¹⁴; an anomalous linear frequency/energy dependency of the electronic scattering rates¹⁵; and a polaronic mode¹⁶. With increasing temperature the low-energy quasiparticle peaks broaden substantially and become incoherent^{9,10}. Under such circumstances the nested Fermi surface with a flat-band feature is expected to be susceptible to electronic instabilities, and indeed charge ordering has been reported around $x \sim 0.5$ ¹⁷. Furthermore, SC states with unconventional/anisotropic order parameters may be expected^{13,18,19,20}. It is therefore important to note that in Na-poor, but still non-hydrated cobaltates ($x \approx 0.3$), charge is more delocalized and the Fermi liquid character of the quasiparticles appears to be recovered with noticeable mass enhancement⁹.

However, very little spectroscopic information has thus far been reported on hydrated, SC cobaltates. Here we report the observation of pronounced electronic Raman scattering (RS) over a wide range of doping levels comprising the SC regime of the phase diagram. This feature uncovers strong carrier scattering by bosonic modes, similar to that observed in underdoped high temperature cuprates. The electronic RS continua in SC and non-SC samples are similar at room temperature, but evolve in a markedly different way as the temperature is lowered. Specifically, a pseudogap opens up below $T \leq T^* \sim 150$ K in SC, but not in non-SC samples. Weak additional phonon modes observed below T^* indicate that the pseudogap may be associated with charge ordering.

Single-crystal samples were prepared in an optical travelling-solvent floating-zone furnace^{21,22}. This is to our knowledge the first systematic RS study of such single crystals that are advantageous due to their easy cleavability and size²³. The experiments ($\lambda=514$ nm,

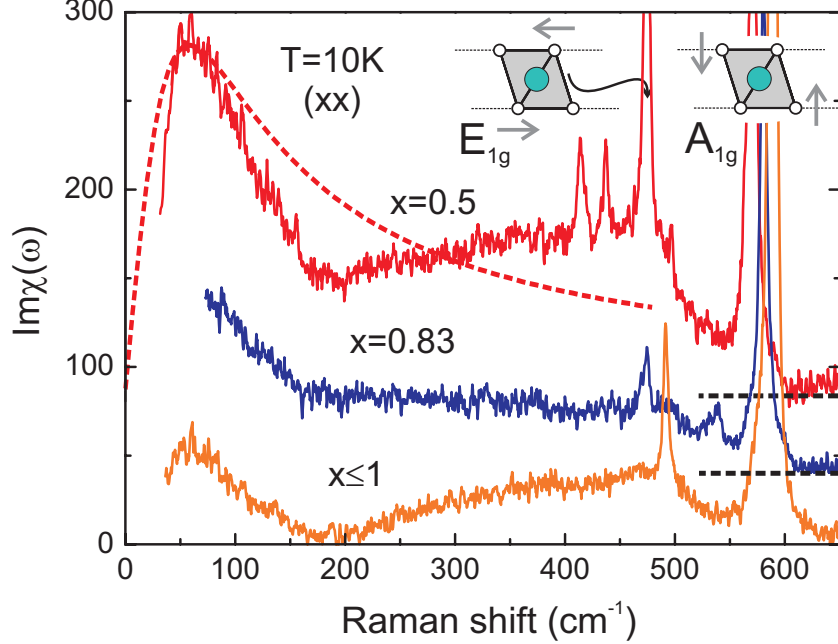


FIG. 1: Raman cross section at $T=10$ K for $x=0.5$, 0.83 , 1.0 with in-plane (xx) light polarization. The insets give oxygen displacements of the main phonon modes using small (bigger) circles for oxygen (cobalt) ions. The curves are shifted for clarity and the dashed lines give an estimate of the background scattering. The curved dashed line corresponds to an electronic RS process with a single, frequency-independent scattering rate, $\Gamma=58$ cm^{-1} , that extrapolates $x=0.5$ at low frequencies.

6 mW, $\varnothing=100\mu m$ diameter laser focus with parallel, in-plane light polarization) were performed in quasi-backscattering geometry on the ab surface of freshly cleaved single crystals. After cleavage, the samples were instantaneously cooled down in He contact gas, in order to prevent dehydration²⁷ or Na ordering at elevated temperatures^{6,28}. We present RS data on four well characterized samples: Three non-SC samples with $y = 0$ and $x = 0.5$, 0.83 , and ≤ 1 , and one SC sample with $x = 0.35$ and $y = 1.3$.

Figure 1 shows the low temperature RS response $Im\chi$ (the measured RS cross section corrected for the Bose thermal population factor) of three non-SC samples with Na content $x = 0.5$, 0.83 , and ~ 1 . All spectra show two strong phonon modes around 580 cm^{-1} and 480 cm^{-1} , which can be attributed to Raman-active out-of-plane A_{1g} and in-plane E_{1g} vibrations, respectively, of oxygen in the CoO_6 octahedra^{24,25}. The eigenvectors are shown as insets in Fig. 1. (Co sites do not contribute to Raman-active lattice vibrations due to their

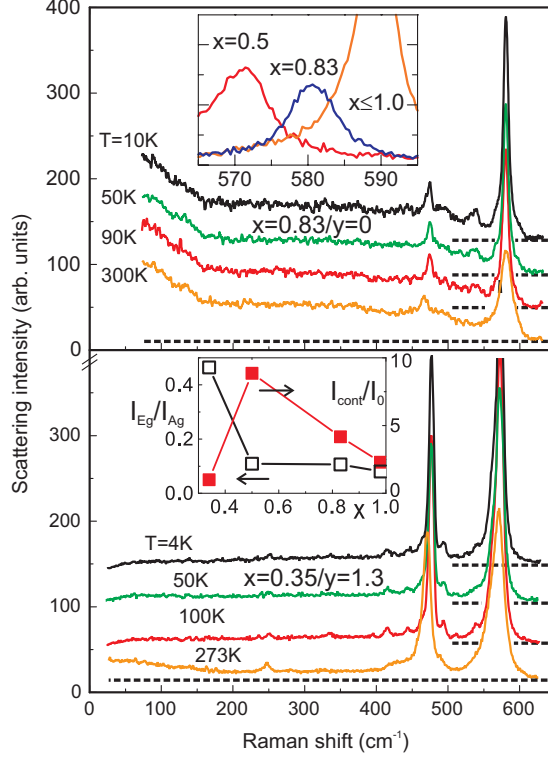


FIG. 2: RS intensity of $\text{Na}_{0.83}\text{CoO}_2$ (upper panel) and $\text{Na}_{0.34}\text{CoO}_2 \cdot 1.3\text{D}_2\text{O}$ (lower panel) in xx light polarization with x in the ab plane of the crystal. The upper inset shows a zoomed view on the out-of-plane A_{1g} mode. The lower inset gives the intensity ratio of the in-plane to the out-of-plane phonon and the integrated intensity of the continuum.

inversion site symmetry.) The sharpness of the higher-frequency mode, whose frequency softens systematically with decreasing x (inset in Fig. 2), testifies to the homogeneity of the samples. The sample with $x = 0.5$, for which Na ordering and a metal-insulator transition have been reported^{6,7}, shows additional modes at 413, 437, and 497 cm^{-1} , close to the energy of the in-plane phonon. This demonstrates the sensitivity of this phonon to structural and electronic ordering processes. In contrast, the sample with $x = 0.83$ exhibits weak modes around 485 and 540 cm^{-1} that might be due to an admixture of inter-plane polarizations, attributable to an E_{2g} mode involving both Na and O motions. Further, note that no anomalous behavior of the phonon modes is observed in frequency and temperature beyond lattice anharmonicities.

The most striking aspect of the spectra shown in Fig. 1 is a continuum with a pronounced, broad peak around $\sim 100 \text{ cm}^{-1}$. Above the peak, the intensity levels off, and

a plateau extends up to about 550 cm^{-1} . Since the crystals are of high quality and show sharp phonon spectra, phonon density-of-states effects can be ruled out as the origin of the continuum. The upper cutoff of the continuum remains at roughly the same energy of 550 cm^{-1} irrespective of Na contents. This is in excellent correspondence with the width of the quasiparticle band determined by photoemission spectroscopy^{9,10} as well as with the knee in the reflectance seen by optical spectroscopy⁷. We hence attribute our observations to electronic RS. Noticeably, the continuum intensity increases nearly monotonically with increasing hole hopping, corresponding to decreasing Na content (lower inset in Fig. 2). This effect corresponds to the increase of the Fermi surface with hole doping that fulfills the Luttinger theorem¹⁰. Deviation seen in the SC sample will be discussed below.

Figure 2 shows in the upper panel the temperature evolution of the RS intensity of antiferromagnetic $\text{Na}_{0.83}\text{CoO}_2$ ($T_N=19.8 \text{ K}$). The data are intentionally presented as raw, non-Bose corrected RS intensity. The weak temperature dependence of the spectra demonstrates that the temperature dependence of the RS scattering cross section approximately compensates the Bose thermal population factor. The lower panel displays electronic Raman scattering in the superconducting sample of composition $\text{Na}_{0.34}\text{CoO}_2 \cdot 1.3\text{D}_2\text{O}$ and superconducting transition temperature $T_{sc}=4.6 \text{ K}$. The overall shapes of the continua are similar at room temperature.

A similar temperature dependence has been observed in RS on high temperature superconductors. The nearly flat, frequency- and temperature-independent continuum has been discussed in the framework of a marginal Fermi liquid state with a linear dependence of the scattering rate on temperature and energy/frequency²⁹. Thus, the unusual temperature dependence of the RS appears to be a consequence of strong electronic correlations as in the high- T_c cuprates. A linear temperature dependence of the scattering rate has also been observed in IR and photoemission experiments on cobaltates^{9,15}. However, there is some important difference. In the cuprates both the electronic RS and the anomalous IR reflectance extend to 0.75 eV . In contrast, the electronic RS of the cobaltates is strongly restricted to a low-frequency region below 550 cm^{-1} ($\approx 0.07 \text{ eV}$). Notwithstanding the generally smaller energy scale, this implies that the observed RS in the cobaltates strongly relies on a mode having an energy scale of 600 cm^{-1} . Remarkably, photoemission and IR spectroscopy measurements give evidence for a bosonic mode of electronic, lattice, or magnetic origin in the same energy range^{7,9,10}. Although further work is necessary to pin down its exact origin, it

is clear that the interaction of charge carriers with a bosonic mode puts constraints to their scattering frequency range. This might be responsible for the low transition temperature in the cobaltates.

We will now focus on the sharply enhanced scattering seen below $\sim 150 \text{ cm}^{-1}$. This energy scale corresponds to the temperature scale at which the quasiparticle dynamics observed by photoemission becomes incoherent. At low frequencies, the lineshape of the RS response of metals and semiconductors can often be approximated by a Lorentzian as function of frequency ω and electronic scattering rate $\Gamma(q, \omega)$: $\text{Im}\chi(\mathbf{q}, \omega) \propto (\omega\Gamma)/(\omega^2 + \Gamma^2)^{30}$. This form provides a reasonable description of the broad low-frequency peaks in the non-hydrated samples (Fig. 1) with a single, frequency independent scattering rate $\Gamma \sim 60 \text{ cm}^{-1}$, not strongly dependent on doping.

We note that similar observations have been made in ferromagnetic semiconductors, e.g. in $(\text{Eu}_{1-x}, \text{Gd}_x)\text{O}$, where the origin of the peak was identified as a magnetic polaron excitation³¹. Further, a similar peak was observed in the infrared spectra of $\text{Na}_{0.82}\text{CoO}_2$ (albeit at a somewhat larger frequency of $\sim 150\text{cm}^{-1}$) and also interpreted as a magneto-polaron mode¹⁶. We hence tentatively ascribe the low-frequency peak in $\text{Na}_{0.5}\text{CoO}_2$ to electronic RS on polarons based on the t_{2g} states of Co. This may indicate that the scattering rate Γ in the samples with lower hole content originates from short-range charge and spin fluctuations, rather than impurities as in conventional semiconductors. Recent neutron scattering data have shown a marked broadening of the spin excitations in a sample with $x = 0.82$ and $y = 0$, consistent with this idea³².

We next address the temperature dependence of the electronic Raman scattering of SC samples. The overall intensity of the continuum (referenced to the intensities of the dominant phonon modes, see lower inset in Fig. 2) is significantly weaker in the hydrated, SC composition than in the non-SC samples. The strong intensity reduction points to a reduced electronic scattering rate, which seems to be inconsistent with more metallic behavior with higher hole doping. This should be ascribed to the fact that Raman spectroscopy is sensitive to the low frequency carrier dynamics and scattering processes without charge conservation. Thus, our Raman data can be interpreted in terms of charge localizations, confirmed below.

The spectra of SC and non-SC samples show a very different evolution as the temperature is lowered. This is highlighted in Fig. 3, where the low-energy $\text{Im}\chi$ is presented for samples with $x=0.35$ and $x=0.83$. At high temperatures both spectra show similar kinks at 185

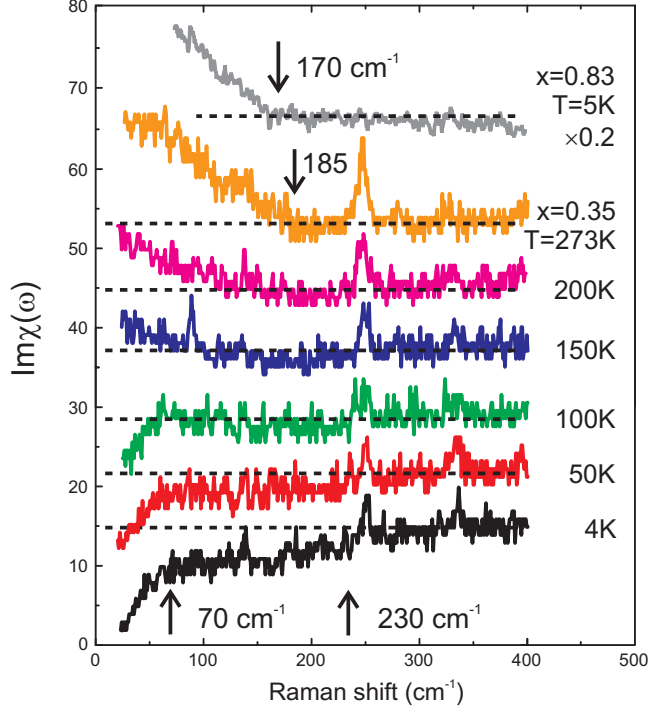


FIG. 3: Low energy RS cross section $Im\chi$ as function of temperature for $Na_{0.35}CoO_2 \cdot 1.3D_2O$. The top curve gives one data set for $x=0.83$ at $T=4K$ scaled by a factor of 0.2. The arrows mark typical energy scales.

and 170 cm^{-1} , respectively. While the kink position is temperature independent in the non-SC sample (Fig. 2a), it shifts to lower energies with decreasing temperature in the SC sample. For $T < 150\text{ K}$, the low-energy spectral weight is sharply suppressed, opening up a “pseudogap” that is not present in samples with $x \geq 0.5$. At 4 K , the spectral depletion is most pronounced at energies below $\sim 70\text{ cm}^{-1}$, but extends up to 230 cm^{-1} , only a factor of two smaller than the high-energy cutoff of the continuum. This implies that the pseudogap energy is not only large compared to the SC transition temperature, but that it constitutes a significant fraction of the energy scales characterizing the electronic structure. The upper panel of Fig. 4 shows that the low-energy scattering rate $\Gamma(T)/\Gamma(273K)$ determined from the inverse of the slope forms a maximum at $T^* \sim 150\text{ K}$ and decreases sharply below this temperature, indicating that the charged quasiparticles become decoupled from the collective excitations. Na ordering and metal-insulator transition for $x=0.5$ ^{6,28} lead to a much more gradual decrease of $\Gamma(T)$.

The experiments presented here are among the first to address electronic excitations in SC

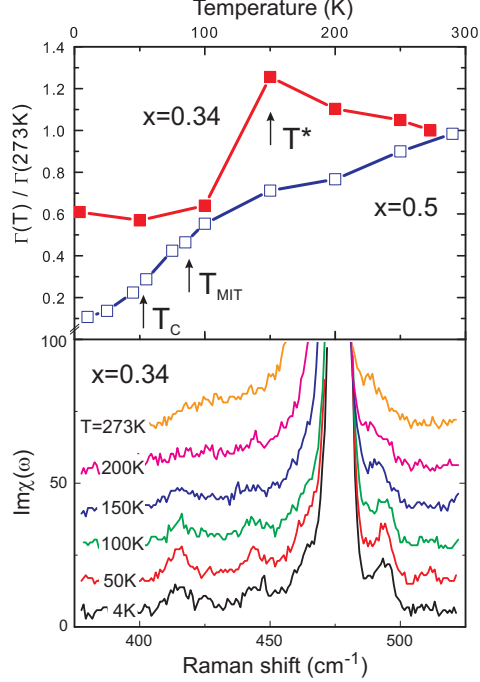


FIG. 4: Normalized electronic scattering rates $\Gamma(T)/\Gamma(273\text{K})$ for $x=0.34/y=1.3$ ($x=0.5/y=0.0$) with full (open) squares with arrows at T^* ($T_{\text{MIT}}=88\text{K}, T_{\text{c}}=53\text{K}$) (upper panel)^{6,28}. The lower panel shows the frequency regime of the E_{1g} phonon with superlattice modes for $T < T^*$.

cobaltates. The reduced intensity of the RS continuum in SC compared to non-SC samples is in general agreement with prior photoemission experiments indicating a crossover from strongly to weakly renormalized quasiparticles with decreasing Na content. Our observation of a pseudogap is also consistent with a recent high-resolution photoemission experiment that has revealed hints of a partial spectral weight depletion in $\text{Na}_x\text{CoO}_2 \cdot y\text{H}_2\text{O}$ in a similar temperature range as that covered by our experiment³⁵.

A clue to the microscopic origin of the pseudogap is provided by the phonon spectrum in the lower panel of Fig. 4. Below T^* , weak sidebands develop close to the in-plane E_{1g} phonon, in a manner similar to the charge-ordered state in $\text{Na}_{0.5}\text{CoO}_2$ (Fig. 1). In contrast, the out-of-plane mode does not couple strongly to the electronic states in the plane. In analogy to the latter material, this effect indicates the formation of a superlattice due to charge ordering. The weak intensity of these modes in the SC sample and their gradual onset point to a very small order parameter in the presence of strong fluctuations³⁴. A related anomaly is observed as an enhanced intensity ratio of the in-plane E_{1g} with respect to the out-of-plane mode (see lower inset of Fig. 2). This is due to a renormalization

of the phonon intensity by a shielding effect of charge carriers and is indeed reciprocal to the intensity of the electronic RS itself. Thus, the origin of the charge ordering instability appears to be predominantly of electronic nature. Evidence of charge ordering has thus far not been reported in SC samples. However, based on model calculations charge ordering has been proposed to be an instability competing with SC^{8,19,21}. In the charge ordered state, the low energy electronic fluctuations related to the Co t_{2g} states at the Fermi energy are expected to be partially suppressed, consistent with our observation¹².

In conclusion, our observation of a low-energy spectral-weight depletion of the electronic RS continuum in SC cobaltates provides evidence for the formation of a pseudogap at temperatures below $T^* \sim 150$ K. Weak phonon anomalies point to the formation of a charge-ordered state below T^* . It is interesting to note that a pseudogap has recently also been observed in the manganite $\text{La}_{1.2}\text{Sr}_{1.8}\text{Mn}_2\text{O}_7$ and attributed to polaron dynamics³⁶. With respect to the cobaltates, however, further experiments are required to assess whether charge order coexists microscopically with SC, or whether the material phase-segregates into SC and charge-ordered states.

We acknowledge discussions with C. Varma, R. Hackl, G. Blumberg, T. P. Devereaux, G. Khaliulin, C. Bernhard, R. Kremer, and Yu. Pashkevich. This work was supported by DFG SPP1073, ESF program *Highly Frustrated Magnetism* (ESF-HFM) and the MRSEC Program of the NSF DMR 02-13282.

-
- ¹ K. Takada *et al.*, Nature **422**, 53 (2003).
 - ² J. D. Jorgensen *et al.*, Phys. Rev. **B 68**, 214517 (2003).
 - ³ J. W. Lynn *et al.*, Phys. Rev. **B 68**, 214516 (2003).
 - ⁴ T. Motohashi *et al.*, Phys Rev. **B 67**, 064406 (2003).
 - ⁵ S. Bayrakci *et al.*, Phys. Rev. **B 69**, 100410 (2004).
 - ⁶ Q. Huang *et al.*, J. Phys: Cond. Matter **16**, 5803 (2004).
 - ⁷ J. Hwang, *et al.*, Phys. Rev. **B 72**, 024549 (2005).
 - ⁸ R. E. Schaak *et al.*, Nature **424**, 527 (2003).
 - ⁹ M. Z. Hasan *et al.*, Phys. Rev. Lett. **92**, 246402 (2004) and cond-mat/0501530 (2005).
 - ¹⁰ H.-B. Yang *et al.*, Phys. Rev. Lett. **92**, 246403 (2004) and Phys. Rev. Lett. **95**, 146401 (2005).

- ¹¹ D. J. Singh, Phys. Rev. **B 61**, 13397 (2000).
- ¹² W. Koshibae and S. Maekawa, Phys. Rev. Lett. **91**, 257003 (2003).
- ¹³ M. D. Johannes *et al.*, Phys. Rev. Lett. **93**, 097005 (2004).
- ¹⁴ I. Terasaki *et al.*, Phys. Rev. **B 56**, 12685 (1997) and Y. Wang *et al.*, Nature **423**, 425 (2003).
- ¹⁵ G. Caimi *et al.*, Europhys. Journ. **B 69**, 213 (2004).
- ¹⁶ C. Bernhard *et al.*, Phys. Rev. Lett. **93**, 167003 (2004).
- ¹⁷ F. L. Ning *et al.*, Phys. Rev. Lett. **93**, 237201 (2004).
- ¹⁸ A. Tanaka and X. Hu, Phys. Rev. Lett. **91**, 257006 (2003).
- ¹⁹ G. Baskaran, Phys. Rev. Lett. **91**, 097003 (2003).
- ²⁰ O. L. Motrunich and P. A. Lee, Phys. Rev. **B 70**, 024514 (2004).
- ²¹ D. P. Chen *et al.*, Phys. Rev. **B 69**, 024506 (2004).
- ²² F. C. Chou, J. H. Cho, and Y. S. Lee, Phys. Rev. **B 70**, 144526 (2004).
- ²³ Earlier RS investigations extensively discuss the effects of degradation^{24,25} or show a phonon spectrum that deviates from the present results²⁶.
- ²⁴ M. N. Iliev *et al.*, Physica **C 402**, 239 (2004).
- ²⁵ P. Lemmens *et al.*, J. Phys.: Cond. Matter **16**, S857 (2004).
- ²⁶ Y. G. Shi *et al.*, Phys. Rev. **B 70**, 052502 (2004).
- ²⁷ M. L. Foo *et al.*, Solid State Commun. **127**, 33 (2003).
- ²⁸ H. W. Zandbergen *et al.*, Phys. Rev. **B 70**, 024101 (2004).
- ²⁹ C. M. Varma *et al.*, Phys. Rev. Lett. **63**, 1996 (1989) and A. Virosztek and J. Ruwalds, Phys. Rev. Lett. **67**, 1657 (1991).
- ³⁰ A. Zawadowski and M. Cardona, Phys. Rev. **B 42**, 10732 (1990) and T. P. Devereaux and A. P. Kampf, Phys. Rev. **B 59**, 6411 (1999).
- ³¹ H. Rho *et al.*, Phys. Rev. Lett. **88**, 127401 (2002).
- ³² S. Bayrakci *et al.*, Phys. Rev. Lett. **94**, 157205 (2005).
- ³³ M. L. Foo *et al.*, Phys. Rev. Lett. **92**, 247001 (2004).
- ³⁴ The modes at 250, 331, 414, 496 cm^{-1} show a $\Delta\omega \approx 80 \text{ cm}^{-1}$ comparable to a typical optical phonon dispersion. The first mode in the proximity to the edge of the depletion has a modified temperature dependence.
- ³⁵ T. Shimojima *et al.*, Phys. Rev. **B 71**, 020505 (2005).
- ³⁶ N. Manella *et al.*, cond-mat/0510423, to appear in Nature (2005).